Boulder Open Space and Mountain Parks

Spatiotemporal Patterns of Algae and Cyanobacteria in Boulder OSMP Waterbodies

Technical Report

March 9th, 2022

Submitted To:

Boulder Open Space and Mountain Parks
Funded Research Program
2520 55th Street
Boulder, Colorado 80301

Submitted By:

Lynker
Nayoung Hur (Lynker, CU Boulder)
Keith Jennings, PhD (Lynker)
Diane McKnight, PhD (CU Boulder)

Lynker

Table of Contents

Figures

Tables

1. Introduction

Algae are important microorganisms, natural to many aquatic ecosystems. They produce oxygen through photosynthesis and serve as food for fish and wildlife. However, with increased nutrient loading and rising water temperature, algae can multiply quickly, causing blooms in slow-moving, warm waters. In some cases, these blooms may be harmful algal blooms (HABs) if they pose certain risks to ecosystems as a result of depleted oxygen levels caused by algal decomposition and/or the presence of toxins harmful to animals and humans. Oftentimes the toxins associated with HABs are produced by cyanobacteria, also known as blue-green algae. News reports and state data from the past several years in Colorado indicate the emergence of HABs as a public health and water quality concern (Brown, 2020; Colorado Department of Public Health and Environment, 2020). At the local level, increased algal growth has been observed in Boulder OSMP waterbodies in the past decade relative to the 1990s and 2000s (Jennings et al., 2021). This is primarily an issue in the summertime when water temperatures are higher, solar radiation is greater, and spring runoff has ceased. This combination can lead to stagnant and stratified water, which increases the opportunity for algal growth (Moore et al., 2008; Clark et al., 2017). To mitigate negative impacts on water quality and to protect human and ecosystem health, it is critical to develop an integrated approach for monitoring algal bloom intensity and timing in Boulder Open Space and Mountain Parks (OSMP) waterbodies.

Such an approach can have several components. For one, *in situ* sampling provides valuable information about water quality parameters including pH, temperature, dissolved oxygen, and conductivity. Additional lab analyses such as measuring chlorophyll-a concentrations in water samples or determining the type of organisms present in a sample via microscopy allow us to quantify algal prevalence (Dörnhöfer and Oppelt, 2016). However, *in situ* sampling can be resource and personnel intensive and may involve delays in sample analysis. Algal blooms and HABs, in particular, are sensitive to many meteorological factors and are considered to be relatively short-lived as algae are easily disturbed (Kutser et al., 2008; Zhao et al., 2020).

> **What's a harmful algal bloom?**
>
> Algal growth may create a harmful algal bloom (HAB) if it meets one of the following criteria:
> 1. Algae consist of cyanobacteria (blue-green algae) that produce toxins
> 2. The algae are so dense that they deplete their waterbody's oxygen supply as they decompose
>
> Importantly, not all algal blooms are harmful and not all cyanobacteria produce illness-causing toxins.

A complementary approach to *in situ* sampling is the use of remote sensing data to evaluate the spatiotemporal patterns of algal blooms. The advantage here is that the data are continuous, frequent, and freely available. Studies have demonstrated that remote sensing analyses can determine the frequency and timing of algal growth and HABs in coastal and inland waters using a series of algorithms (Kahru et al., 1993; Oyama et al., 2015; Ho and Michalak, 2020). There are limits, however, to the applicability of remote sensing data. Their limited temporal and spatial resolutions often determine the type of waterbodies that can be evaluated and at what frequency. Additionally, remote sensing analyses cannot confirm the type of algae present in a given waterbody. Thus, complementing remote sensing products with *in situ* sampling provides a more robust evaluation of algal growth and potential HABs along with the type of algae and cyanobacteria of which they are composed.

Given that OSMP does not currently have a tool for monitoring algal blooms, this study seeks to expand the utility of *in situ* sampling and remote sensing to evaluate algal blooms in Boulder OSMP waterbodies. We used a combination of lab-based and computational methods to answer the following research questions:

- **Question 1:** What type(s) of algae are present in the following waterbodies: Sawhill No. 1, Teller Lake No. 5, Sombrero Marsh, and Wonderland Lake?

- **Question 2:** How do samples of chlorophyll-a and algal type relate to remote sensing algorithm values in the four waterbodies?

2. Methods

To answer our research questions, we used a combination of *in situ* water quality sampling and remote sensing resources to identify summertime algae blooms in four waterbodies managed by Boulder OSMP (Figure 1):

- Sawhill No. 1

- Teller Lake No. 5

- Sombrero Marsh
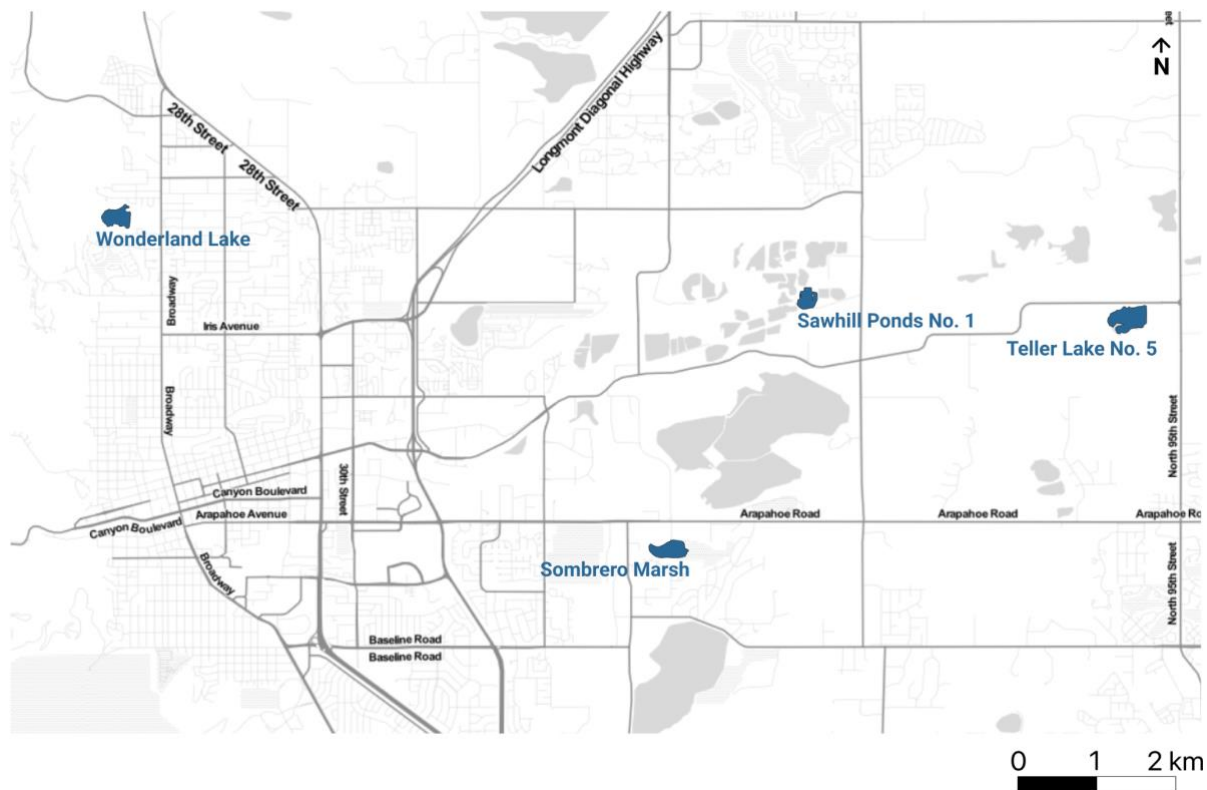
- Wonderland Lake

Figure 1. Overview map of sample sites in Boulder County, Colorado.

Previous OSMP-funded remote sensing research indicated that these waterbodies typically experience algal growth during the summer months (Jennings et al., 2021). An algorithm designed to flag potential cyanobacteria presence also showed that Sawhill No. 1, Teller Lake

No. 5, and Sombrero Marsh may have had HABs in 2019. Remote sensing evidence did not suggest Wonderland Lake experienced an HAB in 2019, but it is a valued community resource with visible algal growth generally lasting from May through September.

To evaluate algal blooms and the presence of cyanobacteria in these waterbodies, we developed a multi-step *in situ* sampling and remote sensing protocol:

1. Collect biweekly water samples in the four waterbodies during Summer 2021
2. Analyze samples in the field and in the lab for various water quality parameters
3. Measure chlorophyll-a concentration in the lab
4. Evaluate the type of algae present with a FlowCam
5. Run a similar remote sensing analysis as in 2021 study
6. Compare water quality and algae data to remote sensing output at the sampling sites

These steps produce the variables defined in Table 1 and are explained in greater detail below.

Table 1. Variables used in this analysis as derived from in situ, lab, and remote sensing data.

Variable	Unit	Instrument	Source	Description
Temperature	°C	Probe	In situ	Water temperature at sampling time
pH	-	Probe	In situ	Measure of how acidic/basic water is at sampling time
Conductivity	mS/cm mSC/cm	Probe	In situ	Measure of collective dissolved ions in the water at sampling time; measure of conductance at a standard 25°C
Dissolved oxygen	mg/L %	Probe	In situ	Measure of oxygen saturation for a given temperature at sampling time
Chlorophyll-a and phaeophytin	mg/L	FluoroMax-3	Lab	Concentration of chlorophyll and phaeophytin in the water sample
Algae type	-	FlowCam	Lab	Type of algae determined through visual identification of FlowCam images
Cyanobacteria count	-	FlowCam	Lab	The absolute and relative number of cyanobacteria in a 5 mL FlowCam sample
NIR:Red ratio	-	Sentinel 2	Remote sensing	Band ratio of near infrared (NIR) to red that provides a continuous range of values that are indicative of algal concentration
FAI-NDWI	-	Sentinel 2	Remote sensing	A two-step algorithm that combines the floating algae index (FAI) and the normalized difference water index (NDWI) to evaluate cyanobacteria as a binary presence/absence

2.1. Field Sampling

We collected water samples from June to mid-August 2021 on a biweekly basis from accessible shoreline locations determined by previous remote sensing data (Figure 2 and Table 2). We took *in situ* field meter measurements at the time of collection for water temperature (°C), pH (unitless), conductivity (mS/cm and mSC/cm), and dissolved oxygen (mg/L and %) using a YSI Model 556 multiparameter sonde. We placed the sonde directly in the water to get these baseline water quality values at each sampling location and time.
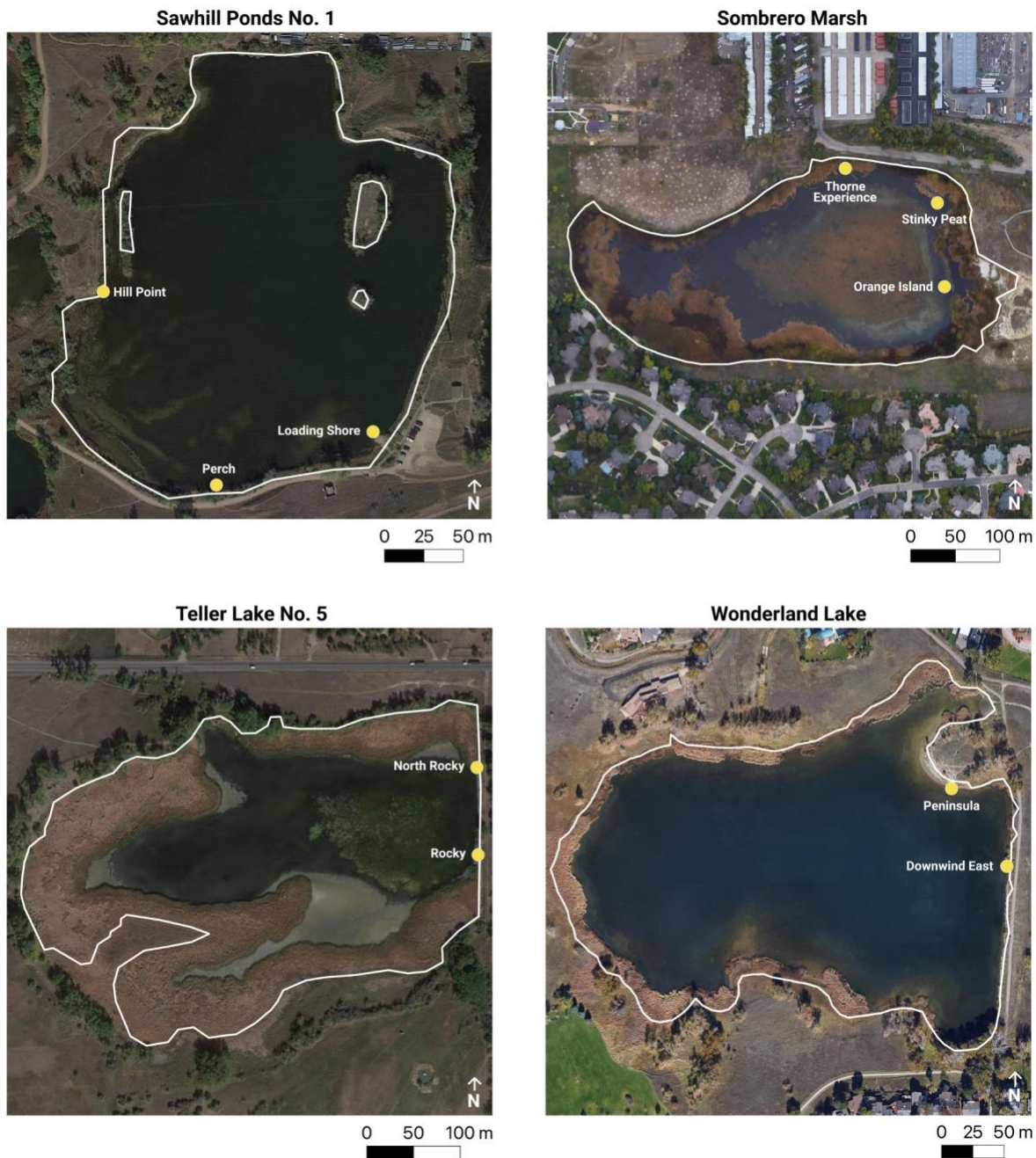

Figure 2. Field sites and sampling locations for each waterbody.

Table 2. Locations and sampling dates for each sampling site. (Note: missing data from 2021-08-09 for Orange Island in Sombrero Mars—we were unable to access the sampling location due to overgrown conditions.)

Waterbody	Sampling site	Coordinates	Sampling dates
Sawhill Pond No. 1	Loading Shore	40°02'22.8"N 105°11'07.6"W	2021-06-01, 2021-06-15, 2021-07-01, 2021-07-13, 2021-07-27, 2021-08-10
	Perch	40°02'21.68" N 105°11'11.77" W	2021-06-01, 2021-06-15, 2021-07-01, 2021-07-13, 2021-07-27, 2021-08-10
	Hill Point	40°02'25.72" N 105°11'14.88" W	2021-06-01, 2021-06-15, 2021-07-01, 2021-07-13, 2021-07-27, 2021-08-10
Sombrero Marsh	Stinky Peat	40°00'43.15" N 105°12'17.87" W	2021-06-01, 2021-06-14, 2021-06-30, 2021-07-12, 2021-07-26, 2021-08-09
	Orange Island	40°00'40.13" N 105°12'17.54" W	2021-06-01, 2021-06-14, 2021-06-30, 2021-07-12, 2021-07-26
	Thorne Experience	40°00'44.40" N 105°12'22.22" W	2021-06-01, 2021-06-14, 2021-06-30, 2021-07-12, 2021-07-26, 2021-08-09
Teller Lake No. 5	North Rocky	40°02'20.68" N 105°08'09.77" W	2021-06-01, 2021-06-14, 2021-07-01, 2021-07-12, 2021-07-26, 2021-08-09
	Rocky	40°02'17.68" N 105°08'09.74" W	2021-06-01, 2021-06-14, 2021-07-01, 2021-07-12, 2021-07-26, 2021-08-09
Wonderland Lake	Peninsula	40°03'2" N 105°17'14" W	2021-05-20, 2021-06-02, 2021-06-15, 2021-06-30, 2021-07-13, 2021-07-27, 2021-08-10
	Downwind East	40°02'60" N 105°17'12" W	2021-05-20, 2021-06-02, 2021-06-15, 2021-06-30, 2021-07-13, 2021-07-27, 2021-08-10

Additionally, we collected approximately 1.0 L of water at each site using 1.0 L clear Nalgene bottles. All Nalgene bottles were rinsed five times with ultrapure deionized water before being used in the field. To ensure representative samples, we rinsed and purged the bottle with the sampling site water twice before filling the bottle a final time with water to be saved for analysis of chlorophyll-a and algae composition. Once we collected the sample, we placed the Nalgene bottle in a labeled bag then stored it in a cooler with an ice pack. All analysis bottles were triple rinsed with ultrapure deionized water. Samples were aliquoted and filtered typically within 3 hours of collection then stored in the lab refrigerator (algae composition) and freezer (chlorophyll-a) until time of analysis. For chlorophyll-a, we used combusted 0.45 μm glass fiber filters, preserving them for later analysis.

2.2. Lab Analysis

2.2.1. Algae Composition

We evaluated algae type using flow-through imaging microscopy. To do this, we first spiked the sample water with 1.0 mL of 5.0% Lugol solution (potassium iodine) to preserve the sample, which we then refrigerated. We next analyzed the preserved samples using the FlowCam, which is a digital imaging flow cytometer designed to rapidly process and identify algal species in a

water sample. FlowCam results have been shown to be comparable to conventional microscopy in previous research (Camoying and Yñiguez, 2016). Here, we determined algae composition by aliquoting 5.0 mL of the sample into the FlowCam. For our FlowCam setup, we used a 10x objective lens which translates to 100x magnification (Figure 3). Per the instrument recommendation, we set the flow rate to 0.150 mL/min yielding 17.5% efficiency, indicating that 17.5% of the volume is imaged. As the sample goes through the FlowCam's flow cell, the instrument recognizes and takes pictures of the specimen. This results in a mixture of identifications, from algae to debris in the water.
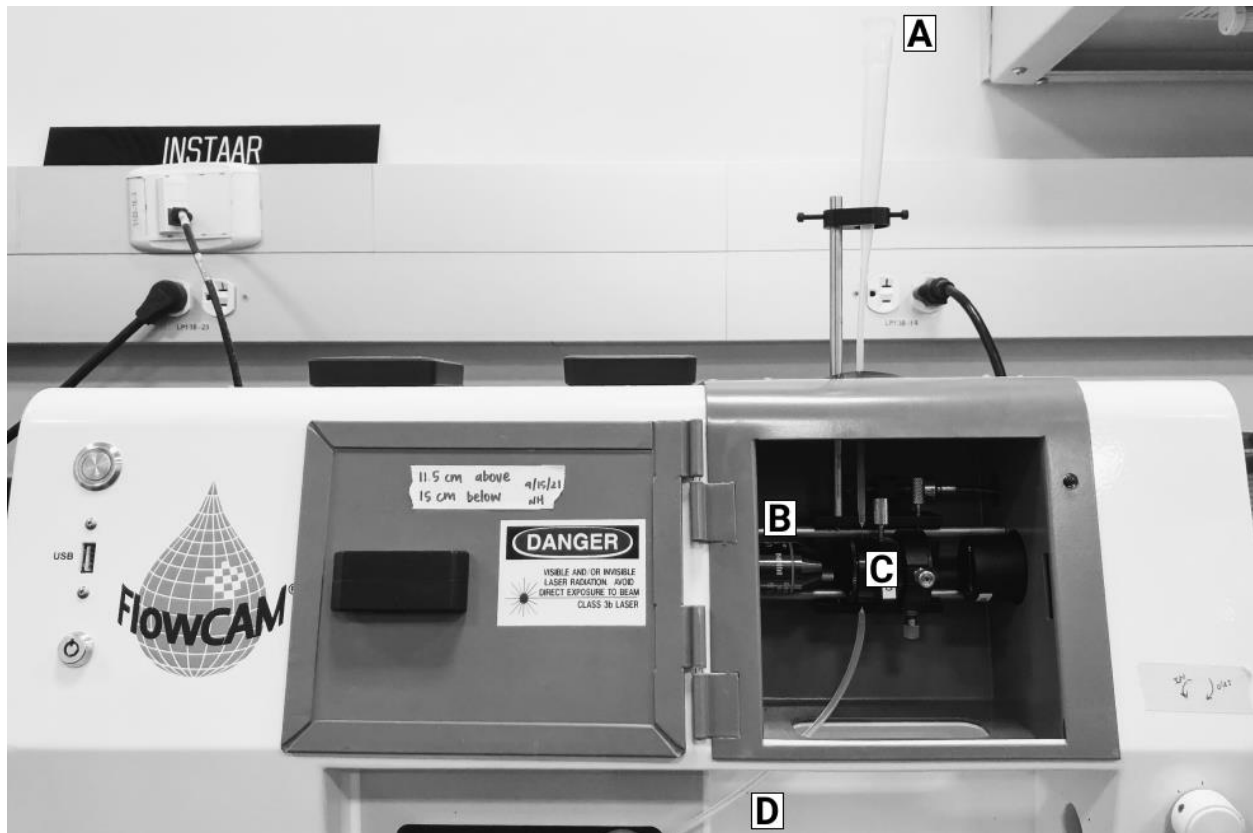
Figure 3. FlowCam setup in the lab. A) 5.0 mL sample fluid input, B) 10x objective lens, C) flow cell, where the sample fluid flows through at 0.150 mL/min with about 17.5% of the specimen captured by the FlowCam, and D) sample fluid discharge/output.

2.2.1.1. *Visual identification to group algae*

The FlowCam outputs individual TIFF files arranged on a grid, typically on micron scales (Figure 4). These images were sorted by date and sampling site. Visual Spreadsheet, a program created by Fluid Imaging, Inc., provides metrics on each FlowCam run. This program estimates biovolume and type of algae once trained with classification data. We first manually sorted through the FlowCam images to obtain general estimates and identified cyanobacteria as well as other organisms in the sample (e.g., green algae and dinoflagellates). Because cyanobacteria are an algal group of concern, particularly when it comes to HABs, we evaluated how much cyanobacteria were found in the water sample with a classification set. Some toxic cyanobacteria are filamentous taxa and we counted predominantly filaments of cyanobacteria which are comprised of varying number of cells. We provide counts as the number of

cyanobacteria filaments and other organisms from all sites for each water body on the day of collection.
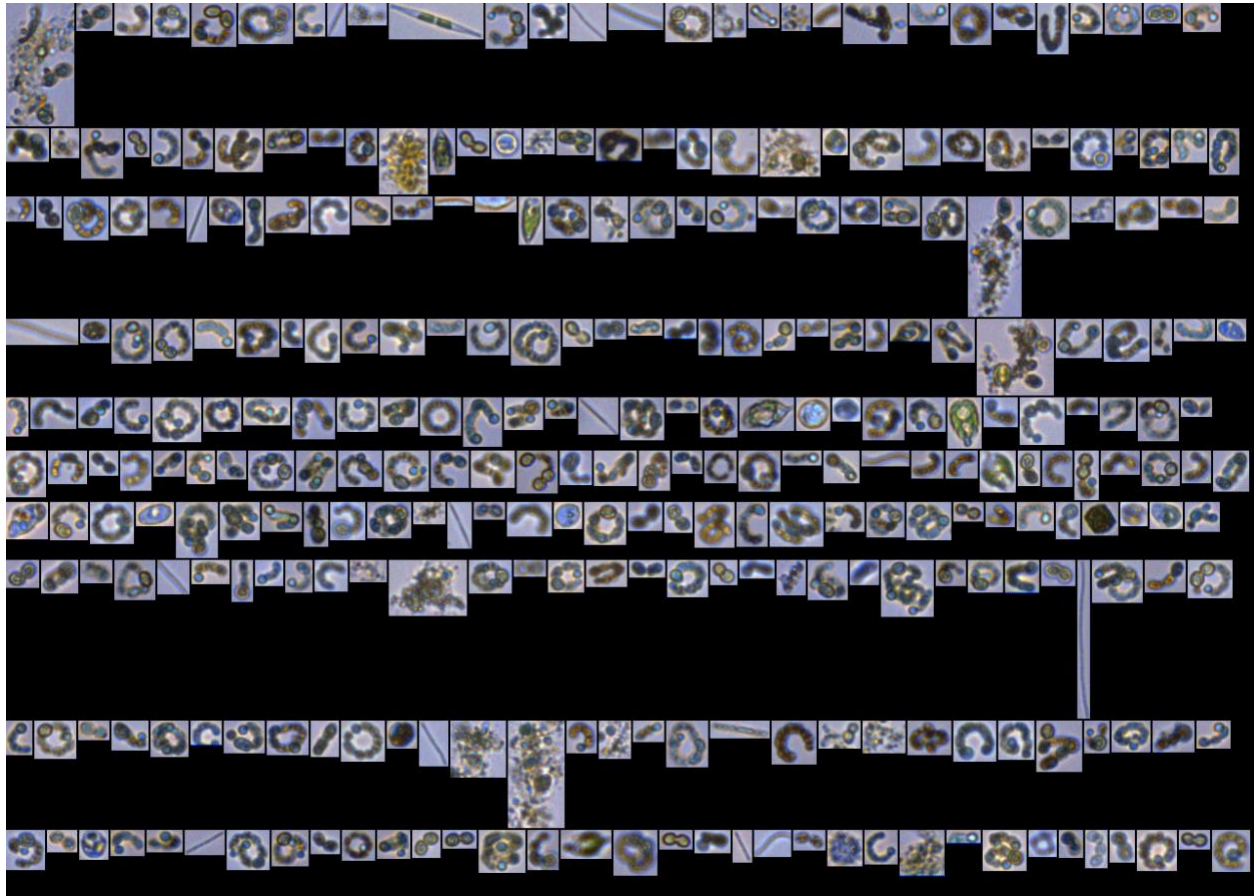
Figure 4. FlowCam output displaying different types of cyanobacteria, diatoms, other algae types, and possibly pollen. Example from 2021-06-30 at Stinky Peat, Sombrero Marsh.

2.2.2. Chlorophyll-a and Phaeophytin

Chlorophyll-a is the green pigment found in both cyanobacteria and other types of algae that allows them to photosynthesize. In general, as the amount of algae increases, so does the concentration of chlorophyll-a in a water sample, making it a key indicator of algal bloom magnitude. All sample preparation and measurement for chlorophyll-a was performed in a darkened room to prevent the degradation of photosynthetic pigments. We filtered approximately 100 mL of the sample water from each site. The combusted glass fiber filters were wrapped in foil and then frozen until 2 days before sample analysis. The frozen wrapped filters were thawed for a minimum 24 hours at room temperature, then placed in a glass vial wrapped in aluminum foil with 20 mL 90% buffered acetone and set in a refrigerator for 24 hours to allow pigment extraction. We measured each sample twice with the Horiba FluoroMax-3 fluorometer, the first measurement for chlorophyll-a, and the second measurement with the solution spiked with 0.1 M HCl for phaeophytin. Phaeophytin is a compound formed with the degradation of chlorophyll-a. This derivative can indicate senescence of algal communities with light energy being converted to chemical energy, so we expect a semi-positive relationship between phaeophytin and chlorophyll-a values; while the concentrations for chlorophyll-a and

phaeophytin follow similar trends, when chlorophyll-a values are high, the phaeophytin values may be lower and vice versa.

The fluorometer outputs two intensities: S_a and S_b, which are after acid and before acid, respectively. We can then compute concentrations using the following equations:

$$[Chl\text{-}a](ug/L) = Cf\left(\frac{r}{r-1}\right)(S_{b-blank} - S_{a-blank})(V_a/V_s) \qquad \text{(Eq. 1)}$$

$$[Phaeophytin](ug/L) = Cf\left(\frac{r}{r-1}\right)\left[(r \cdot S_{a,blank}) - S_{b,blank}\right](V_a/V_s) \qquad \text{(Eq. 2)}$$

where Cf refers to the calibration factor (which is the slope of S_b vs. the calculated chlorophyll concentrations of the diluted standards determined by a spectrophotometer; $Cf = 0.0493$), r is the average ratio of S_b/S_a ($r = 4.80$), $S_{a-blank}$ and $S_{b,blank}$ are to the intensities minus the blank measured from calibration, V_a is the volume of acetone added to extract the pigment ($V_a = 0.02\ L$), and V_s is the volume of the sample filtered.

2.3. Remote Sensing

2.3.1. Image Processing

In addition to the *in situ* sampling, we extended the remote sensing analysis from the previous study, focusing on just the 2021 waterbodies of interest. To do this, we analyzed high-resolution optical imagery from the Sentinel 2A and 2B satellites, which offer several advantages over other instruments, including a finer spatial resolution (10 m versus 30 m for Landsat) and shorter repeat times between satellite overpasses (2 to 5 days). Specifically, we accessed the Sentinel 2 Level 1-C Top of Atmosphere product using the Google Earth Engine processing platform (Gorelick et al., 2017). These data come in a series of bands, each of which corresponds to a specified range of wavelengths in the electromagnetic spectrum that is detected by a given sensor on the satellite. This is analogous to the camera in your smartphone, which captures data in red, green, and blue bands. As befits a $200 million satellite, the Sentinel 2 sensor (Table 3) captures a great deal more information than a smartphone camera. The large number of Sentinel 2 bands allows us to use detection algorithms that evaluate the presence of both green algae and cyanobacteria.

Table 3. Sentinel 2 band information. Note: there are slight differences, typically less than 10 nm, between Sentinel 2A and 2B (https://sentinel.esa.int/web/sentinel/user-guides/sentinel-2-msi/resolutions/radiometric).

Band	Name	Spectral Range (nm)	Spatial Resolution (m)
1	Coastal Aerosol	432–453	60
2	Blue	458–523	10
3	Green	543–578	10
4	Red	650–680	10
5	Red Edge 1	698–713	20
6	Red Edge 2	733–748	20

7	Red Edge 3	773−793	20
8	NIR	785−899	10
8a	Narrow NIR	855−875	20
9	Water Vapor	935−955	60
10	SWIR1	1358−1389	60
11	SWIR2	1565−1655	20
12	SWIR3	2100−2280	20

In this project we used the two algae algorithms we evaluated in our previous report. The first algorithm ratios the reflectance (i.e., the proportion of incoming radiation reflected to the satellite sensor) of the near infrared (NIR) and red bands. The NIR:Red ratio is close to zero for clear water and increases with algae concentrations (Tebbs et al., 2013). We also used a rule-based algorithm to evaluate cyanobacterial presence using two other remote sensing metrics, the Floating Algae Index (FAI) and the Normalized Difference Water Index (NDWI):

$$FAI = R_{NIR} - \left[R_{Red} + (R_{SWIR1} - R_{Red}) \times \frac{(865 - 655)}{(1610 - 655)} \right] \qquad \text{(Eq. 3)}$$

$$NDWI = \frac{(R_{NIR} - R_{SWIR1})}{(R_{NIR} + R_{SWIR1})} \qquad \text{(Eq. 4)}$$

where R represents the top of atmosphere reflectance (0−1) for a given band (e.g., R_{NIR} is the reflectance value for the NIR band). Compared to the simple NIR:Red ratio, the algorithm based on FAI and NDWI is slightly more complex, employing two thresholds in a rule-based scheme to estimate the presence of a cyanobacterial bloom (Oyama et al., 2015). First, the FAI differentiates between clear water and algae using a threshold of 0.05. The FAI considers values greater than or equal to 0.05 to be algae, while those below are clear water. Next, the NDWI partitions algae (i.e., pixels with FAI ≥ 0.05) into cyanobacteria and non-cyanobacteria blooms using a threshold of 0.63. Values greater than or equal to this threshold are considered probable cyanobacterial blooms while those below are not.

We applied the above algorithms to the Sentinel 2 data in Google Earth Engine to evaluate temporal and spatial patterns of algae presence and potential cyanobacterial blooms. To do this, we used similar analysis methods as in our previous report. For each *in situ* sampling location (Table 2), we created three types of data extraction points: edge, near-edge, and open-water. Each extraction point type corresponds to a remote sensing pixel next to or co-located with the *in situ* sampling location. This lets us isolate the actual (edge) or potential (near-edge) overlap of the remote sensing imagery with the waterbody edge. We include output from all three types because a mixture of land and water in a remote sensing pixel will influence algorithm output compared to open-water pixels, but algae are more likely to concentrate near the shore. Once we had created the extraction points, we then used Google Earth Engine to access all Sentinel 2 data between April 1st and October 1st, 2021 at these locations, removing days when clouds obscured the earth's surface from the satellite sensor. With these data, we

created a time series of the NIR:Red ratio and the FAI-NDWI cyanobacteria algorithm at each extraction point.

In addition to the time series data, we also created maps for each waterbody showing the number of times each pixel exceeded a NIR:Red ratio greater than 1 and met the conditions for cyanobacteria according to the FAI-NDWI algorithm. This was done in a slightly different manner than the time series data extraction described in the previous paragraph. For this part of the analysis, we stepped through each day of Sentinel 2 data and calculated the NIR:Red ratio and ran the FAI-NDWI algorithm across every pixel in Boulder County. We created two new maps, one corresponding to each algorithm. We added 1 to each pixel in the maps whenever the NIR:Red or FAI-NDWI thresholds were respectively exceeded in that pixel on a cloud-free day with Sentinel 2 data. The final products were the two maps, masked to the waterbodies of interest, showing the number of times each pixel within a given waterbody exceeded a NIR:Red ratio greater than 1 and met the conditions for cyanobacteria according to the FAI-NDWI algorithm.

2.3.2. Remote Sensing to *In Situ* Data Comparison

We also evaluated whether the NIR:Red ratio output showed any mathematical relationship to the *in situ* sampling of chlorophyll-a concentrations. To do this, we associated each *in situ* sample of chlorophyll-a to the corresponding average NIR:Red ratio value for that open water sampling location within ±15 days of the sampling date to account for noise in the sensor data as well as infrequent valid Sentinel 2 data as a result of cloud cover and overpass timing. We then plotted the remotely sensed NIR:Red ratio against the chlorophyll-a concentration and computed a line of best fit to determine the mathematical relationship between the two. We also created a mixed effects model with waterbody as the random effect to understand the control waterbody exerts on the relationship between the NIR:Red ratio and chlorophyll-a.

We additionally analyzed whether cyanobacteria detected by the FlowCam corresponded to cyanobacteria indicated by the FAI-NDWI algorithm. Here, we associated *in situ* cyanobacteria presence/absence (when the number of FlowCam-detected cyanobacteria exceeded 5) with whether the FAI-NDWI algorithm had indicated blue-green algae presence at any time within ± 15 days. We then computed the number of true positives (yes-yes), true negatives (no-no), false positives (yes-no), and false negatives (no-yes) of the remote sensing detection algorithm compared to the *in situ* data.

3. Results

3.1. Field Sampling—Water Quality Parameters Over Time

Our *in situ* sampling showed that water temperatures fluctuated over time (Figure 5), which is consistent with expectations in a shallow water habitat. Deep water has greater thermal inertia, meaning it changes temperature slower than shallow water. At the OSMP waterbodies, this means warm days can bring about large increases in water temperature, as observed in the change between June 1st and June 15th. At some locations the jump in water temperature exceeded 5°C.
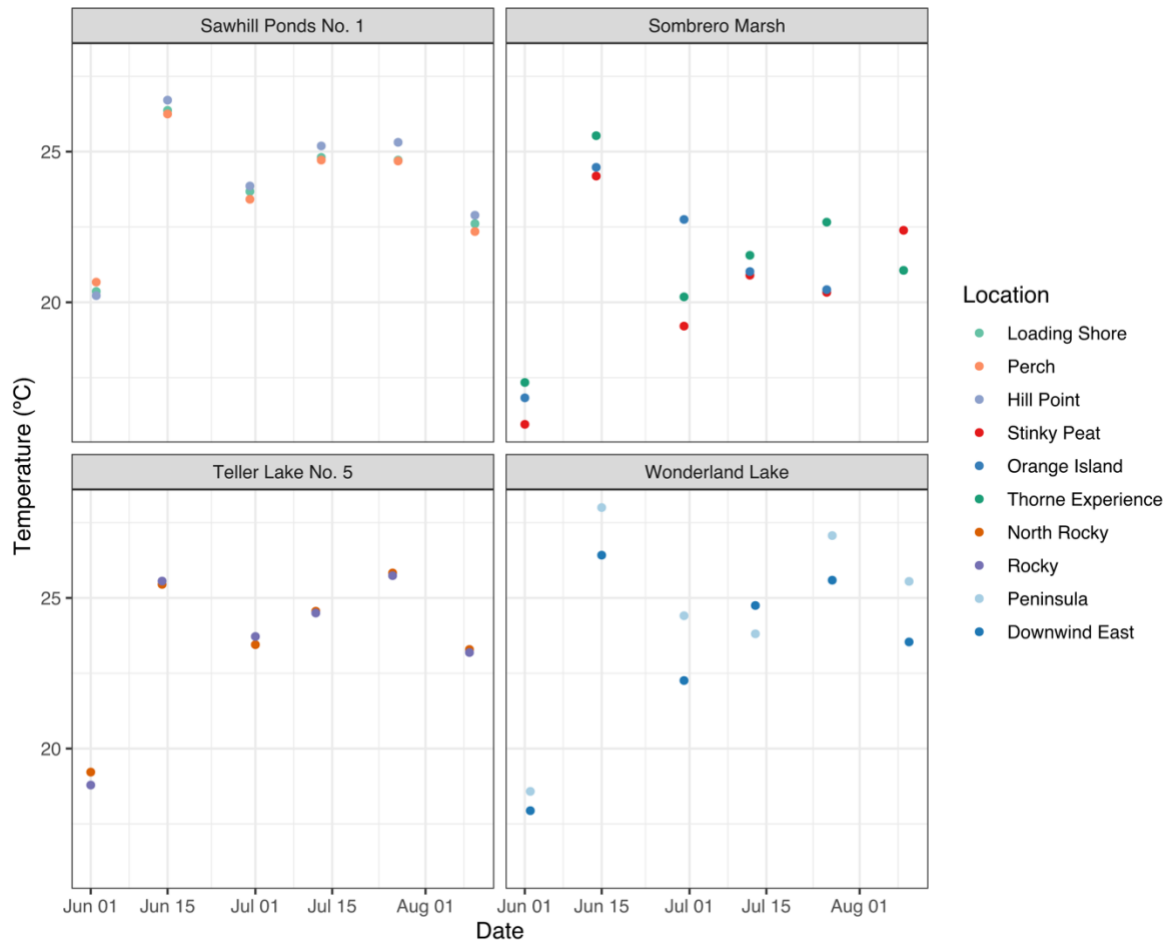
Figure 5. Water temperature measured in situ *over time at each waterbody and sampling location.*

pH remained alkaline in all waterbodies (Figure 6) with Sawhill Ponds No. 1 being the most alkaline. Across all sampling sites, Sawhill Ponds No. 1 had a range from 9.47 to 12.87 with Loading Shore exhibiting higher pH values. For Sombrero Marsh the pH ranged from 8.37 to 11.96, Teller Lake No. 5 pH ranged from 7.99 to 10.65, and Wonderland Lake pH ranged from 7.96 to 11.39. For these waterbodies, all sampling sites fell within similar pH ranges of each other. Measured high pH values could occur due to depletion of dissolved CO_2 and lack of reaeration with the atmosphere, a characteristic of eutrophic water bodies in the summer.
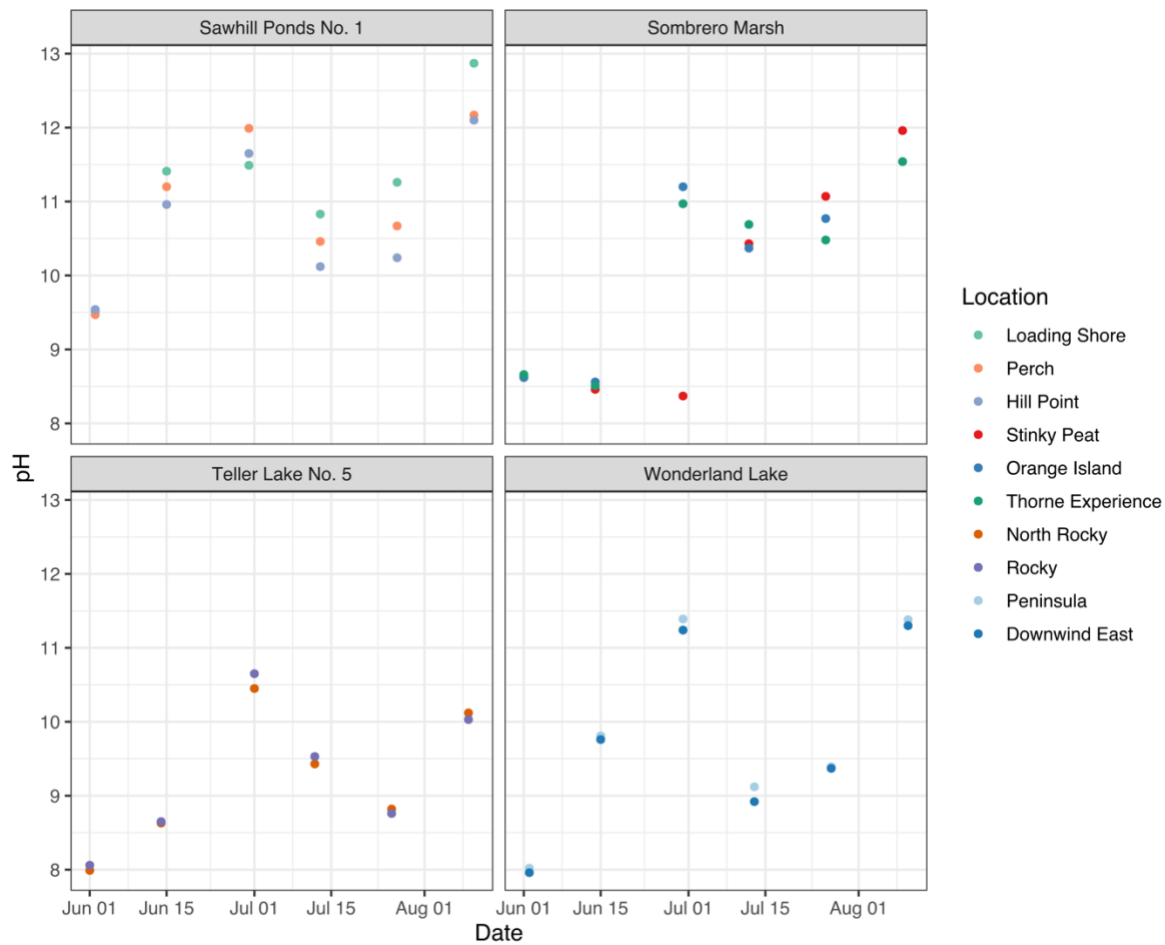
Figure 6. pH measured in situ *over time at each waterbody and sampling location.*

Sombrero Marsh had the highest specific conductivity values (Figure 7), ranging from 4374 μSºC/cm to 6986 μSºC/cm. Wonderland Lake had the second highest readings, approximately a quarter of what we observed at Sombrero Marsh. Sawhill No. 1 and Teller Lake No. 5 both had specific conductivity readings roughly an order of magnitude lower than the other two waterbodies.
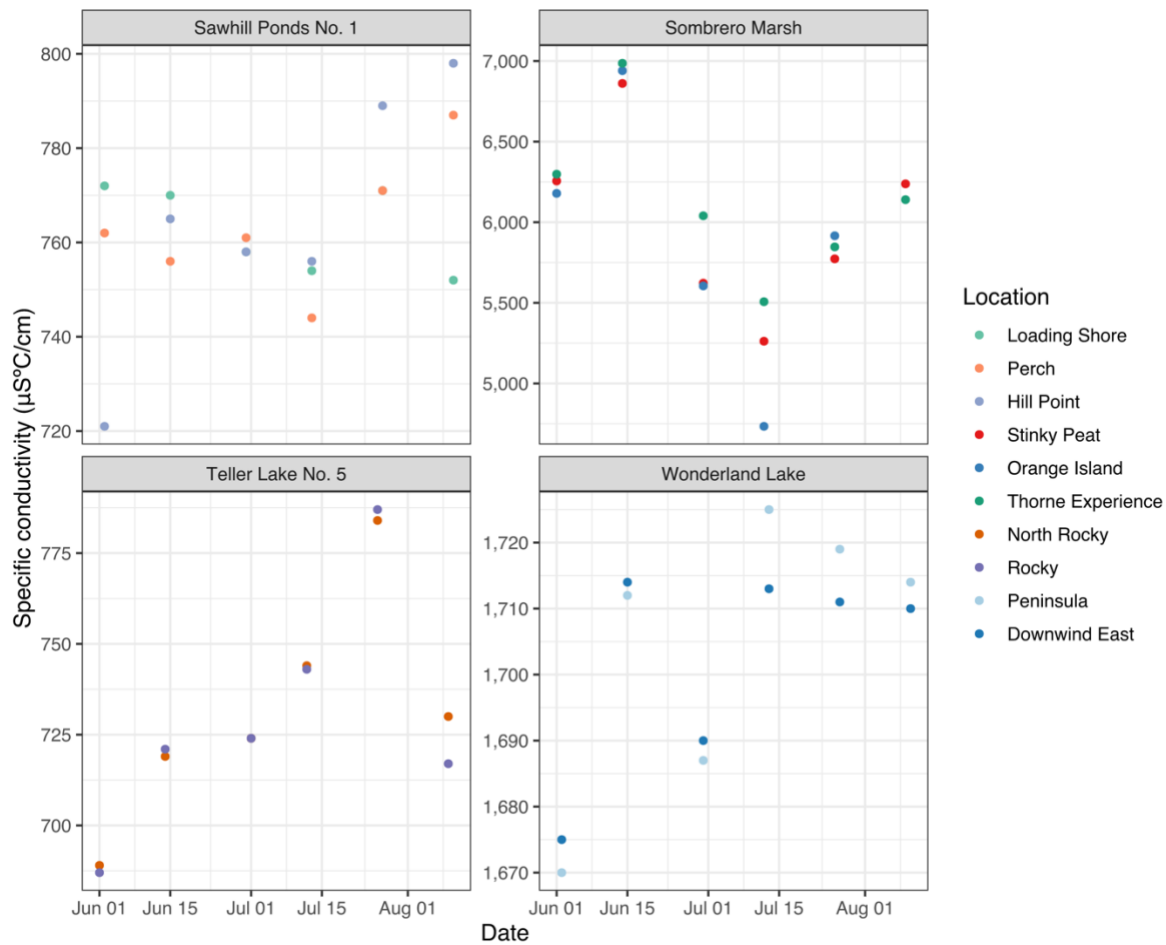
Figure 7. Specific conductivity measured in situ over time at each waterbody and sampling location.

Similarly, Sombrero Marsh had the largest range for DO from 0.03 mg/L (0.4%) to 20.32 mg/L (225.6%) (Figure 8 and Figure 9). At Sawhill Ponds No. 1, Hill Point generally had the lowest DO among all other sampling sites. For Teller Lake No. 5, the DO ranged from 4.75 mg/L (55.7%) to 9.33 mg/L (114.2%). Wonderland Lake exhibited a higher range from 5.96 mg/L (73.2%) to 10.0 mg/L (124.0%). Relative DO values larger than 100% are indicative of dissolved gases in the surface waters not being in equilibrium with the overlying atmosphere. Two likely causes of this are (1) active photosynthesis (typically from algae) and (2) rapid changes in temperature that lead to non-equilibrium with water and air, so the oxygen is "trapped" in the water at time of sampling. Sombrero Marsh exhibits higher DO values than other waterbodies, which we attribute this to the visually observed cyanobacterial bloom (Figure 10).
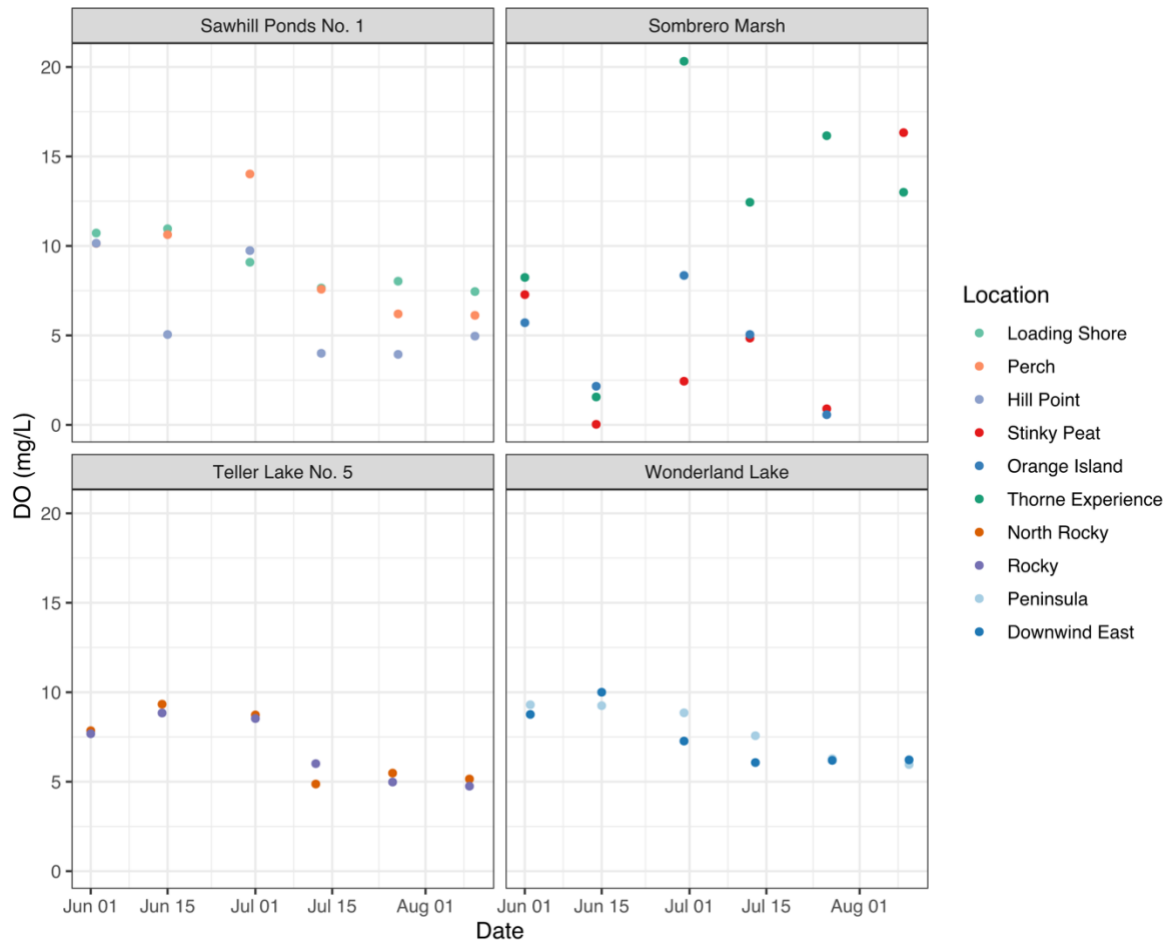
Figure 8. Dissolved oxygen (DO) measured in situ *over time at each waterbody and sampling location.*
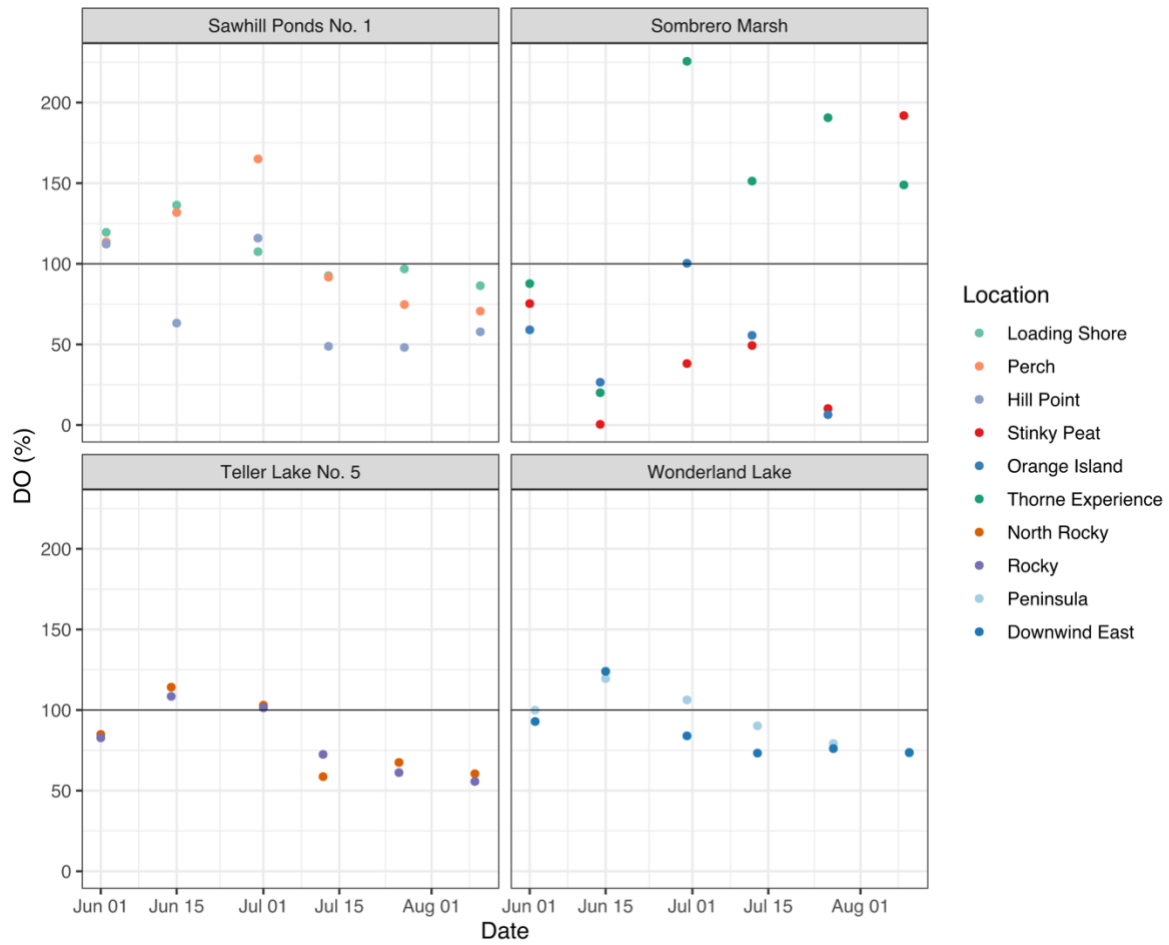
Figure 9. Dissolved oxygen (DO) measured in situ over time at each waterbody and sampling location.

Figure 10. Visible cyanobacteria blooms in Sombrero Marsh on 2021-08-09.

3.2. Lab Analysis

3.2.1. Algae Types by Location and Time

According to the FlowCam, there were a variety of algae types, including cyanobacteria, in the four sampled waterbodies. Pictured below (Figure 11), the types we found were blue-green algae, green algae, dinoflagellates, and golden algae.

Figure 11. Algae types found via FlowCam. Note: the photos are not to scale.

The types of algae varied over time and by waterbody (Table 4). Beginning in July, Sawhill Ponds No. 1 had cyanobacteria including *Dolichospermum* (Anabaena) and *Spirulina*. Other algae found were *Ceratium* (dinoflagellate), *Phacus* (green), *Closterium* (green), *Staurastrum* (green), and *Cosmarium* (green).

Sombrero Marsh had cyanobacteria at the start and end of the sampling campaign, with higher abundance beginning in late June. Identified cyanobacteria were *Dolichospernum* (Anabaena), *Oscillatoria*, *Spirulina*, and *Mycrosystis*. The dominant genus was *Dolichospernum* (Anabaena), and its abundance peaked mid-to-late July.

By mid-to-late July, water samples from Teller Lake No. 5 began showing cyanobacteria presence. *Dolichospermum* (Anabaena) were the most dominant cyanobacteria, but *Oscillatoria* and *Aphanizomenon* were also present. Golden and green algae were also present throughout the sampling period.

Wonderland Lake had very few (< 5 photos) cyanobacteria present in June and early July but reached noticeably higher counts at the end of July and August (Figure 12). Other algae found were *Ceratium* (dinoflagellate), *Desmodesmus* (green), and other filamentous green algae (few identified in the order Zygnematales). Green algae primarily dominated Wonderland Lake, as they were present in the waterbody starting May, identified by FlowCam results and visual inspection.

Table 4. Algae presence in the waterbodies as determined with the FlowCam.

Waterbody	Type	Taxonomic group	Occurrence
Sawhill Pond No. 1	Dinoflagellate	*Ceratium*	June – July
	Green	*Closterium*, *Staurastrum*	June – August
	Blue-green	*Dolichospermum* (Anabaena)	July – August
Sombrero Marsh	Blue-green	*Dolichospermum* (Anabaena), *Oscillatoria*, *Spirulina*	June – August
	Green	*Phacus*, *Strombidium*	June – August
Teller Lake No. 5	Blue-green	*Dolichospermum* (Anabaena)	Mid-July – August
	Golden	*Dinobryon*	June – August
Wonderland Lake	Dinoflagellate	*Ceratium*	June – July
	Blue-green	*Dolichospermum* (Anabaena)	Begins June, increases mid-July – August
	Green	*Desmodesmus*, Zygnematales	June – August

FlowCam results indicate that biomass, defined as the count of organisms in a given volume (5 mL for this study), generally increased throughout the summer either peaking at the end of July or early August (Figure 12). At the beginning of the sampling season, biomass counts were in the hundreds, then reached thousands in July for Sombrero Marsh and in late July for Wonderland Lake. We further investigated into cyanobacteria and its presence throughout the

sampling period. Sombrero Marsh had the highest counts and thus percentage of cyanobacteria biomass (Figure 12 and Figure 13).
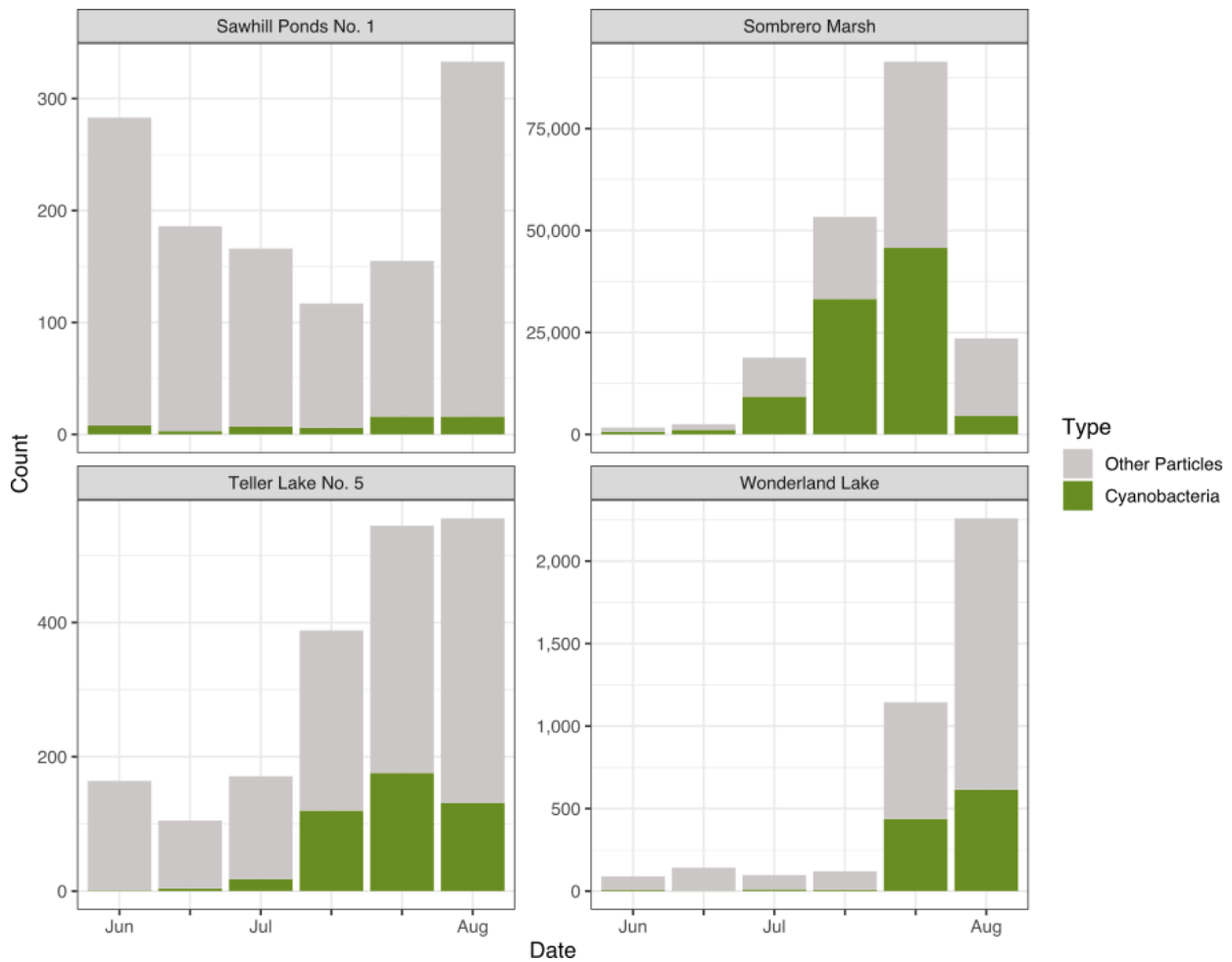
Figure 12. Counts from the FlowCam of total particles summed across sampling locations each waterbody split into two categories – other particles (organisms other than cyanobacteria) and cyanobacteria. Note the different y-axis scales.
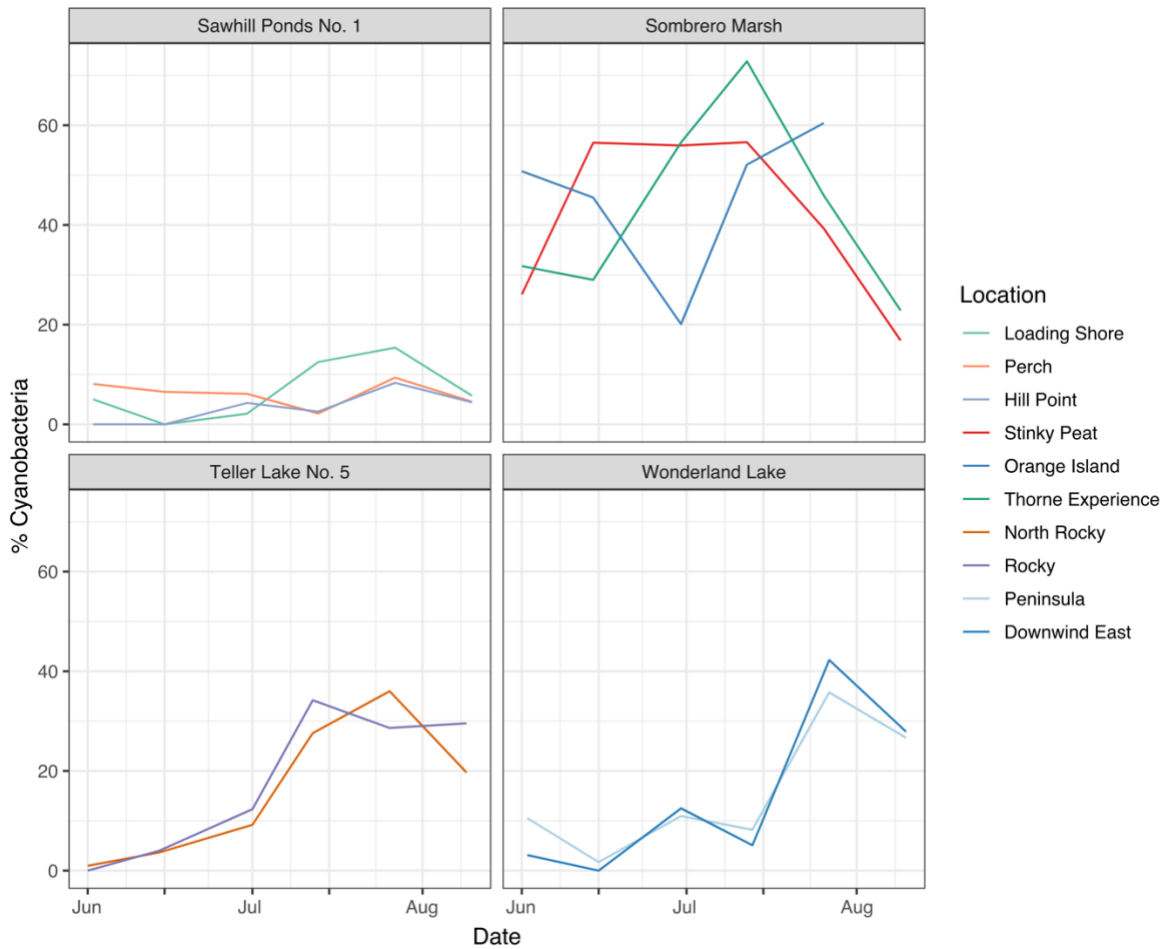
Figure 13. Time series of percent cyanobacteria in water sample.

3.2.2. Chlorophyll-a and Phaeophytin Over Time

Results from the fluorometer indicate that the phaeophytin concentrations were higher in the early summer, with chlorophyll-a dominating later in the summer (Figure 14). Sombrero Marsh had the highest chlorophyll-a and phaeophytin concentrations among all the sampled waterbodies, over an order of magnitude greater than the others. Chlorophyll-a values at Sawhill Ponds No. 1 were lower than all the water bodies with maximum concentrations less than 3 µg/L. Teller Lake No. 5 and Wonderland Lake both had maximum chlorophyll-a values less than 20 µg/L, while Sombrero Marsh reached a peak of near 300 µg/L at the end of August.
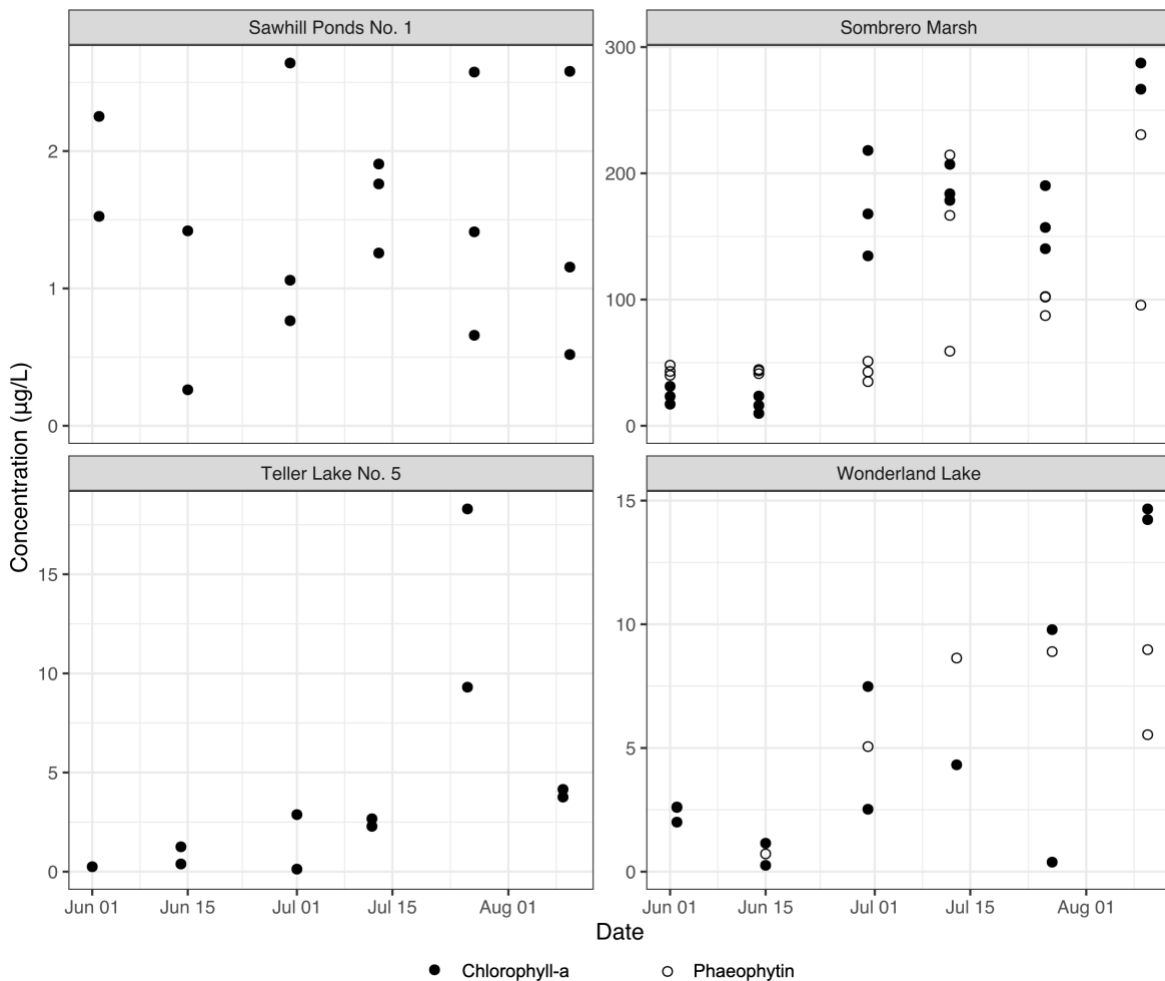
Figure 14. Chlorophyll-a and phaeophytin concentrations for all sampling sites for each location from June to August, concentrations not detected by fluorometer are omitted. Note the different y-axis scales.

3.3. Remote Sensing Analysis

3.3.1. NIR:Red and FAI-NDWI Over Time

According to the NIR:Red remote sensing data, all four waterbodies expressed evidence of algae growth in 2021 (Figure 15), consistent with the *in situ* findings. For each location and pixel type, the NIR:Red ratio exceeded 1 for at least several satellite overpasses. In general, the NIR:Red ratio increased from a minimum in early spring to a maximum in late summer. The seasonal pattern was most pronounced at Sombrero Marsh, where all locations showed a clear cycle of algae growth (increasing NIR:Red values) and senescence (decreasing NIR:Red values). The pattern was relatively muted at Wonderland Lake, indicating a lower degree of algal growth during the summer months. Open water pixels typically had the lowest NIR:Red values, indicating either greater algae growth for the edge and near edge pixels or potential effects of shoreline vegetation on algorithm output.
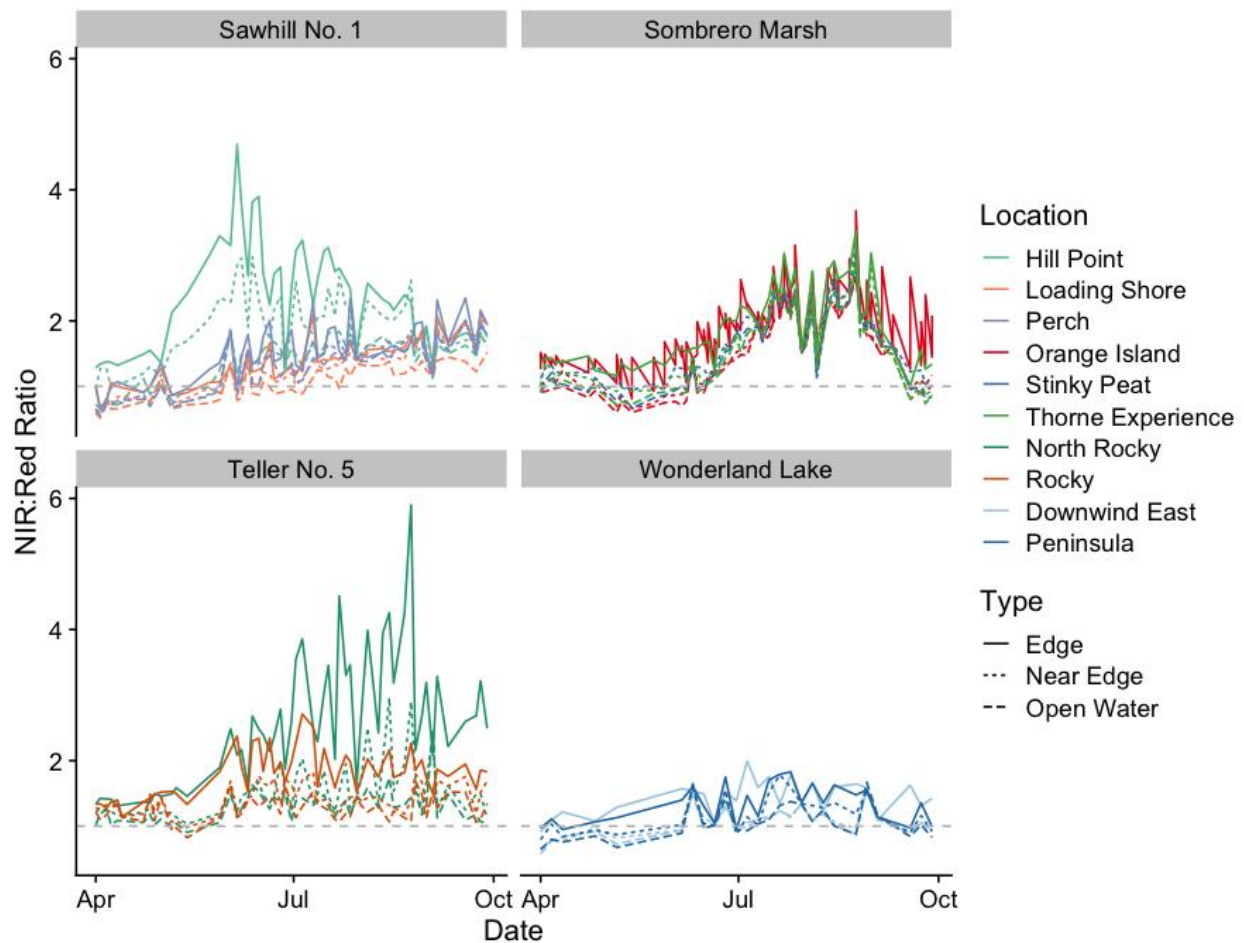
Figure 15. 2021 time series of the NIR:Red ratio at each sampling location and pixel type for the four waterbodies in our analysis. The gray dashed line corresponds to a NIR:Red value of 1. Traces above this line are consistent with algae growth.

The story is different for the FAI-NDWI algorithm, which indicated consistent cyanobacteria presence only at analyzed locations in Sombrero Marsh (Figure 16). Although the NIR:Red ratio increased at most sites starting in late spring, the FAI-NDWI algorithm did not show potential blue-green algae growth until July. Also of note is the fact that open water and near edge pixels typically expressed higher cyanobacterial contents than the edge pixels, which may have been a result of the NDWI reducing edge effects by partitioning values into either vegetation (< 0.63) or blue-green algae (>= 0.63).
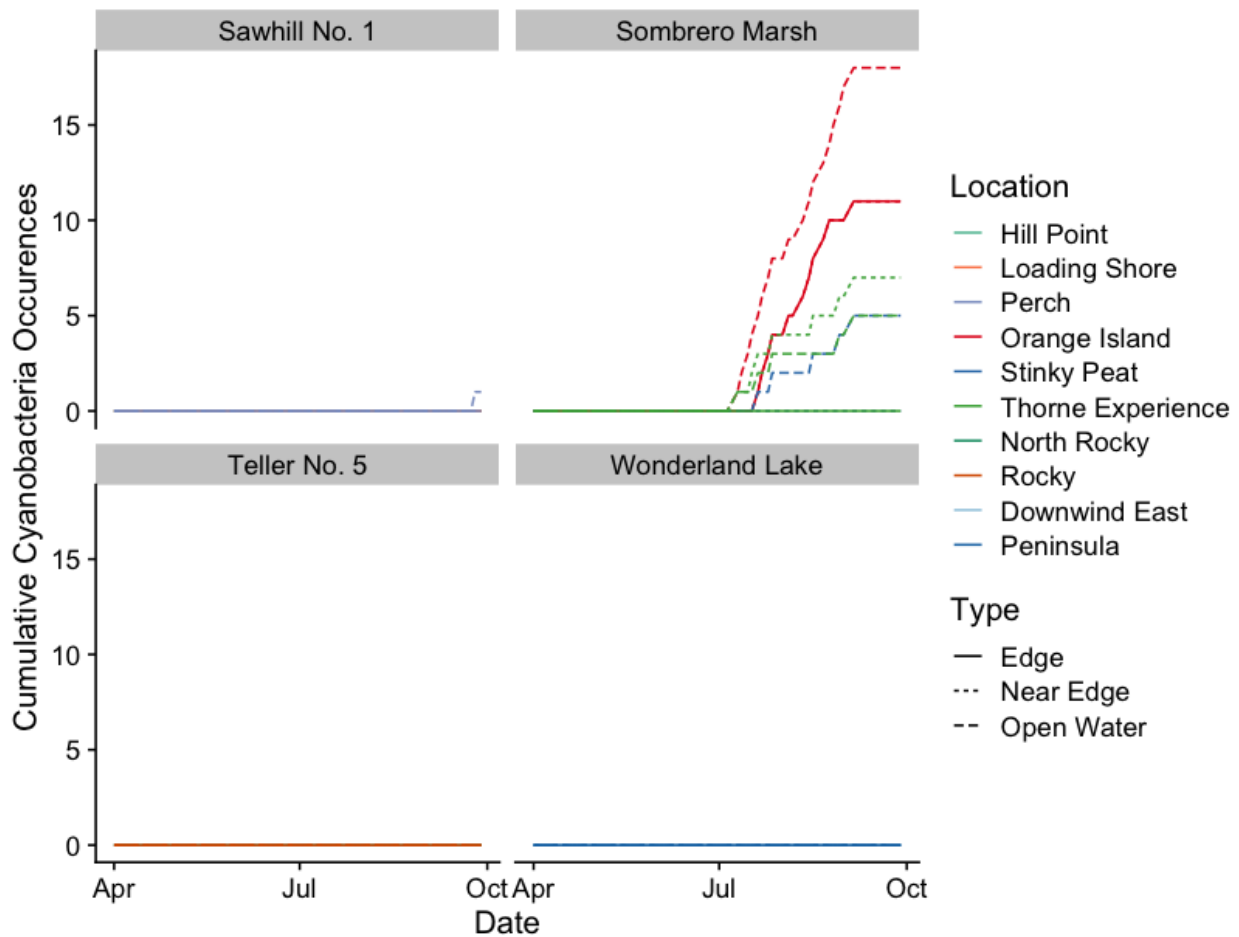
Figure 16. 2021 cumulative cyanobacteria occurrences based on the FAI-NDWI algorithm at each sampling location and pixel type for the four waterbodies in our analysis

3.3.2. NIR:Red and FAI-NDWI exceedance maps

Similar to the results above, all four waterbodies presented consistent evidence of algal growth according to maps showing the number of times each pixel within their boundaries recorded a NIR:Red value greater than 1. In contrast, maps of FAI-NDWI output suggested that 3 of the 4 waterbodies had cyanobacteria present, whereas the time series results above indicated only Sombrero Marsh did. According to its maps, Sombrero Marsh (Figure 17) had marked algal growth and likely cyanobacteria blooms throughout most of its open water area. Sawhill No. 1 (Figure 18) and Teller Lake No. 5 (Figure 19) also had likely extensive algal blooms according to their NIR:Red ratio maps, but they expressed a smaller area of potential blue-green algae compared to Sombrero Marsh. Notably, the area of potential cyanobacteria at these two waterbodies did not overlap with the edge, near edge, and open water pixels corresponding to the *in situ* sampling points. Wonderland Lake (Figure 20), in contrast to the other three, had a lower number of NIR:Red values > 1 and no occurrences of potential cyanobacteria according to the FAI-NDWI algorithm.

Figure 17. The number of exceedances counted using the NIR:Red threshold (left) and the FAI and NDWI thresholds (right) from April 1st 2021 through October 1st 2021 at Sombrero Marsh. The greater the number of exceedances, the more persistent a probable algal or cyanobacterial bloom may be. Satellite imagery: © 2021 Google, CNES / Airbus, Maxar Technologies, Public Laboratory, U.S. Geological Survey, USDA Farm Service Agency.

Figure 18. The number of exceedances counted using the NIR:Red threshold (left) and the FAI and NDWI thresholds (right) from April 1st 2021 through October 1st 2021 at Sawhill No. 1. The greater the number of exceedances, the more persistent a probable algal or cyanobacterial bloom may be. Satellite imagery: © 2021 Google, CNES / Airbus, Maxar Technologies, Public Laboratory, U.S. Geological Survey, USDA Farm Service Agency.

Figure 19. The number of exceedances counted using the NIR:Red threshold (left) and the FAI and NDWI thresholds (right) from April 1st 2021 through October 1st 2021 at Teller Lake No. 5. The greater the number of exceedances, the more persistent a probable algal or cyanobacterial bloom may be. Satellite imagery: © 2021 Google, CNES / Airbus, Maxar Technologies, Public Laboratory, U.S. Geological Survey, USDA Farm Service Agency.

Figure 20. The number of exceedances counted using the NIR:Red threshold (left) and the FAI and NDWI thresholds (right) from April 1st 2021 through October 1st 2021 at Wonderland Lake. The greater the number of exceedances, the more persistent a probable algal or cyanobacterial bloom may be. Satellite imagery: © 2021 Google, CNES / Airbus, Maxar Technologies, Public Laboratory, U.S. Geological Survey, USDA Farm Service Agency.

3.4. Remote Sensing to *In Situ* Data Comparison

We found mixed results when comparing lab-measured chlorophyll-a values to the NIR:Red ratio at each sampling location and time. Across all waterbodies, there was a statistically significant positive relationship between the two variables. Although there was a large amount of scatter in the values, we computed an r^2 of 0.57 and a *p-value* of less than 0.0005. The slope of the best-fit line was 189.2, indicating that an increase in the NIR:Red ratio of 1 was associated with a 189.2 µg/L increase in the chlorophyll-a concentration. However, when we examined the waterbodies individually (Figure 21), only chlorophyll-a and NIR:Red values from Sombrero Marsh had a statistically significant relationship (p < 0.0005), with an r^2 of 0.80 and a slope of 182.9. All other per-waterbody relationships were not statistically significant.
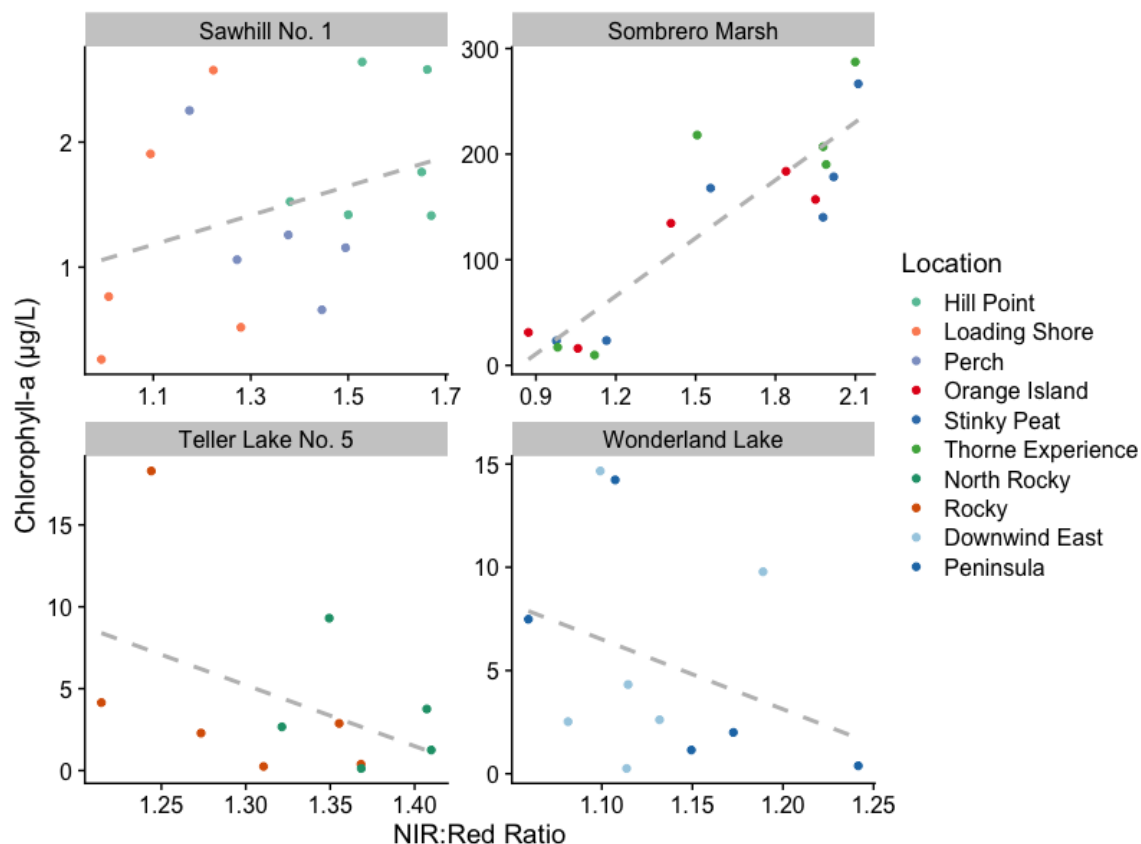
Figure 21. Comparison of the remotely sensed NIR:Red ratio to lab-tested values of chlorophyll-a from the four waterbodies. The grey line is the line of best fit at each waterbody. The slope of the best fit line is only statistically significant (p < 0.05) at Sombrero Marsh.

To further assess the likelihood of location-specific relationships, we ran a linear mixed effect model with random effects. This model explored the relationship between chlorophyll-a and the NIR:Red ratio as a fixed effect, with waterbody as a random effect. The results indicated that the waterbody explains 67% of the variance, meaning which waterbody we sampled has a moderate effect on the relationship between the NIR:Red ratio derived from remote sensing and lab-tested values of chlorophyll-a (Table 5). The slope and intercept of the relationship are both statistically significant, with the former being slightly smaller than the slope computed using ordinary least squares regression across all of the waterbodies.

Table 5. Linear mixed effect model summary results with waterbody as the random effect.

Coefficients	Estimates	CI	p
Intercept	-156.99	-218.54 – -95.44	<0.001
NIR:Red (slope)	143.69	113.13 – 174.25	<0.001
Random Effects			
Variance, σ^2	1012.05		
Residual, τ_{00}	2029.09		
Intraclass correlation coefficient, ICC	0.67		
$N_{waterbody}$	4		

Waterbody	Intercept
Sawhill No. 1	-189.46355
Sombrero Marsh	-94.26036
Teller Lake No. 5	-186.49839
Wonderland Lake	-157.73723

Relative to FlowCam-observed cyanobacteria, the remote sensing FAI-NDWI algorithm only expressed a 52.5% accuracy. It correctly predicted 10 true positives and 21 true negatives, which were when the algorithm and FlowCam (cyanobacteria count >= 5) both indicated cyanobacteria presence or absence, respectively. The algorithm produced 28 false negatives, suggesting no cyanobacteria were present when the FlowCam indicated that they were. There were no false positives, suggesting the algorithm was relatively conservative and that low cyanobacteria counts from Teller Lake No. 5, Sawhill No. 1, and Wonderland Lake were difficult to detect.

4. Discussion

4.1. Synthesis

In this study, the combination of *in situ* sampling and remote sensing provided an integrated approach to monitoring algae blooms in Boulder OSMP waterbodies. Compared to our remote sensing project in 2020, the addition of water quality sampling enabled a more robust analysis. We found that algae became more prevalent in each waterbody as summer progressed, according to both the chlorophyll-a concentrations and remote sensing results. Of the four waterbodies, Sombrero Marsh had the greatest lab-measured chlorophyll-a concentrations, over an order of magnitude greater than the others. Its remotely sensed NIR:Red ratio values were also generally higher than the other waterbodies, particularly when evaluating the open water pixels.

In the laboratory, we observed several types of algae via the FlowCam, including blue-green, green, and golden algae as well as dinoflagellates. Similar to the chlorophyll-a analysis, Sombrero Marsh expressed the greatest amount and most frequent occurrences of cyanobacteria when examining FlowCam imagery. Interestingly, the other three waterbodies all showed evidence of cyanobacteria presence during the 2021 summer sampling season, generally increasing after mid-to-late July. According to the remotely sensed FAI-NDWI algorithm time series output, only Sombrero Marsh expressed evidence of cyanobacteria presence. However, the exceedance maps suggested a different story, with Sawhill No. 1 and Teller Lake No. 5 both showing clear patterns of cyanobacteria blooms. This highlights the shortcomings of sampling and testing a selection of locations—the spatiotemporal variability of algal blooms calls for comprehensive monitoring across space and time. Neither the remotely sensed time series nor map data showed cyanobacteria for Wonderland Lake, for example.

When we compared the remote sensing data to the laboratory data, we found varying levels of performance. In general, across all waterbodies, we saw an increase in the concentration of

chlorophyll-a with higher NIR:Red values. This indicates that for our sites, the remotely sensed ratio does detect algal concentrations, although there is a fair bit of scatter. We suggest that the NIR:Red ratio could be used to assess the presence of algal blooms, but would likely have considerable uncertainty if used to predict specific chlorophyll-a concentrations.

The FAI-NDWI time-series algorithm tended to be relatively conservative in detecting cyanobacterial presence. It had a 52.5% accuracy and there were no false positives (detecting cyanobacteria when the FlowCam data showed none). The FAI-NDWI maps did slightly better, showing cyanobacteria in three of the four waterbodies in which they were observed in the FlowCam. Here, the combination of approaches shows a much more complete picture of cyanobacterial patterns than any method used on its own.

4.2. Assumptions and Limitations

Chlorophyll-a concentrations can be influenced by a variety of factors. One is light intensity, meaning concentrations often fluctuate on a diurnal basis due to photoinhibition of phytoplankton. All of our *in situ* sampling occurred between 8:00 AM and 12:00 PM MDT, which does not capture the diurnal cycle of solar radiation and chlorophyll-a. The geographic location of the sampling site can also affect the measured water quality parameters (Was the site shaded?) and so can prevailing meteorological conditions (Was there cloud cover on the day of sampling? Did it rain the day before/day of sampling?). While most of our sampling days did not have rain, our field notes indicate that half the sampling days had sunny skies and the other half had overcast skies. 2021-06-01, 2021-06-02, 2021-07-01, and 2021-07-26 were sunny, but on these days it had rained within the previous 24 hours.

Remote sensing approaches are also subject to important assumptions and limitations, such as waterbody size, mixed land-water pixels, and atmospheric effects (cloud cover, haze). We also imposed empirically derived thresholds for determining cyanobacteria blooms. Such thresholds may not work for all waterbodies in different geographic regions. For example, we found that the FAI-NDWI maps detected cyanobacterial blooms that the time series analysis did not. This expected behavior, caused by the inherent variability in cyanobacteria patterns, underscores the need for a multi-faceted approach to monitoring HABs. Overall, the algorithm may not be as sensitive to cyanobacteria presence as we would like. The lack of false positives suggests it is relatively conservative, underreporting potential blooms. Another concern is that cyanobacteria can move within a water column. Many cyanobacteria species have gas vacuoles that allow them to regulate their buoyancy, meaning cyanobacteria can move from the surface to lower depths that satellite sensors may not be able to measure.

Additionally, the regressions we performed on NIR:Red to chlorophyll-a data showed weak relationships at all sites except for Sombrero Marsh. This waterbody had both the highest maximum (287 μg/L) and the largest range in chlorophyll-a concentrations in 2021. These values put Sombrero Marsh on the low side of data presented in previous literature. Tebbs et al. (2013), for example, regressed chlorophyll-a concentrations approaching 700 μg/L against band ratio values nearing 3.5 as computed from remote sensing data. Similarly, Oyama et al. (2015) evaluated remote sensing output from waterbodies with chlorophyll-a concentrations between 174 and 21736 μg/L. Thus, relative to other work, algal concentrations in the sampled waterbodies are relatively low. This is important because water absorbs much of the incoming shortwave radiation emitted by the sun, which causes satellite sensors to report a greater amount of noise relative to the signal returned by low over-water reflectances. Functionally, this means waterbodies with denser algal blooms (i.e., greater chlorophyll-a concentrations), such

as Sombrero Marsh, return a more reliable signal. The NIR:Red ratio is therefore a less reliable indicator of absolute chlorophyll-a values in waterbodies with low chlorophyll-a concentrations.

4.3. Management Implications

For both the lab-based and remote sensing approaches, we were unable to assume that the detected cyanobacteria were toxic. Only lab analyses for toxicity can determine this, whether it is detecting certain cyanotoxins or performing eDNA on water samples. However, these lab tests are expensive, costing approximately $100-200 per sample. In a resource- and time-limited system, monitoring algal blooms will likely requiring a multi-step approach that leverages the best aspects of each method. Remote sensing can quickly provide information on the spatiotemporal patterns of algal blooms and HABs, while *in situ* sampling can produce more granular information on water quality, chlorophyll-a concentrations, and algae type. As an additional step, Boulder OSMP may want to use the findings of this and the previous report as a guide to which waterbodies should receive additional toxicity testing in the coming years.

5. Conclusions

This study tracked the evolution of algal blooms in four Boulder OSMP waterbodies using *in situ* testing, laboratory analyses, and remote sensing data. The main findings are as follows:

- Lab-measured chlorophyll-a concentrations increased from spring through late summer
  - Peak concentrations were an order of magnitude higher at Sombrero Marsh than at the others

- FlowCam imagery revealed a variety of algae at the four waterbodies, including blue-green, green, and golden algae as well as dinoflagellates
  - Cyanobacteria were found at all waterbodies and were most prevalent at Sombrero Marsh; the finding of cyanobacteria does not necessarily mean cyanotoxins were present

- Remote sensing data showed an increasing NIR:Red ratio from spring to late summer, corresponding to algal growth at the four waterbodies

- Time series values of the FAI-NDWI algorithm indicated cyanobacteria presence only at sampling locations in Sombrero Marsh
  - Maps from algorithm output, however, showed additional blue-green algal blooms also at Teller Lakes No. 5 and Sawhill No. 1

- The remote sensing algorithms had a variable relationship to lab-measured values
  - The NIR:Red ratio had a positive, statistically significant relationship with chlorophyll-a concentrations only at Sombrero Marsh
  - The FAI-NDWI algorithm underpredicted cyanobacterial blooms and recorded no false positives

Overall, we found utility in all examined approaches, each of which provided information to better understand algal blooms and HABs in Boulder OSMP waterbodies. Future monitoring efforts may also include lab analyses of toxicity to fully quantify the risks to human and animal health.

6. Acknowledgments

Boulder Open Space and Mountain Parks provided the award that funded this study. We are grateful to OSMP's Marianne Giolitto, who supplied invaluable guidance and data in support of this project. We also thank OSMP's Dr. Brian Anacker for his feedback on a draft of this report.

7. Citations

Brown, J. (2020). Filling Colorado Lakes with Slimy Pea-Green Soup. Are Hotter Summers Making It Worse? *Colo. Sun*. Available at: https://coloradosun.com/2020/08/20/toxic-algae-in-colorado-lakes/.

Camoying, M. G., and Yñiguez, A. T. (2016). FlowCAM optimization: Attaining good quality images for higher taxonomic classification resolution of natural phytoplankton samples. *Limnol. Oceanogr. Methods* 14, 305–314. doi:10.1002/lom3.10090.

Clark, J. M., Schaeffer, B. A., Darling, J. A., Urquhart, E. A., Johnston, J. M., Ignatius, A. R., et al. (2017). Satellite monitoring of cyanobacterial harmful algal bloom frequency in recreational waters and drinking water sources. *Ecol. Indic.* 80, 84–95. doi:10.1016/j.ecolind.2017.04.046.

Colorado Department of Public Health and Environment (2020). HAB dashboard. Available at: https://cohealthviz.dphe.state.co.us/t/EnvironmentalEpidemiologyPublic/views/newhab_draft/HABdash?:showAppBanner=false&:origin=viz_share_link&:display_count=n&:showVizHome=n&:isGuestRedirectFromVizportal=y&:embed=y [Accessed January 10, 2021].

Dörnhöfer, K., and Oppelt, N. (2016). Remote sensing for lake research and monitoring - Recent advances. *Ecol. Indic.* 64, 105–122. doi:10.1016/j.ecolind.2015.12.009.

Gorelick, N., Hancher, M., Dixon, M., Ilyushchenko, S., Thau, D., and Moore, R. (2017). Google Earth Engine: Planetary-scale geospatial analysis for everyone. *Remote Sens. Environ.* 202, 18–27.

Ho, J. C., and Michalak, A. M. (2020). Exploring temperature and precipitation impacts on harmful algal blooms across continental U.S. lakes. *Limnol. Oceanogr.* 65, 992–1009. doi:10.1002/lno.11365.

Jennings, K. S., Wlostowski, A. N., and Hur, N. J. (2021). Tracking the Historical Prevalence of Algal Blooms in Boulder Waterbodies Using Satellite Imagery. Boulder, CO.

Kahru, M., Leppanen, J.-M., and Rud, O. (1993). Cyanobacterial blooms cause heating of the sea surface. *Mar. Ecol. Prog. Ser.* 101, 1–7.

Kutser, T., Metsamaa, L., and Dekker, A. G. (2008). Influence of the vertical distribution of cyanobacteria in the water column on the remote sensing signal. doi:10.1016/j.ecss.2008.02.024.

Moore, S. K., Trainer, V. L., Mantua, N. J., Parker, M. S., Laws, E. A., Backer, L. C., et al. (2008). Impacts of climate variability and future climate change on harmful algal blooms and

human health. *Environ. Health Glob. Access Sci. Source* 7, 1–12. doi:10.1186/1476-069X-7-S2-S4.

Oyama, Y., Matsushita, B., and Fukushima, T. (2015). Distinguishing surface cyanobacterial blooms and aquatic macrophytes using Landsat/TM and ETM+ shortwave infrared bands. *Remote Sens. Environ.* 157, 35–47. doi:10.1016/j.rse.2014.04.031.

Tebbs, E. J., Remedios, J. J., and Harper, D. M. (2013). Remote sensing of chlorophyll-a as a measure of cyanobacterial biomass in Lake Bogoria, a hypertrophic, saline–alkaline, flamingo lake, using Landsat ETM+. *Remote Sens. Environ.* 135, 92–106.

Zhao, Y., Liu, D., and Wei, X. (2020). Monitoring cyanobacterial harmful algal blooms at high spatiotemporal resolution by fusing Landsat and MODIS imagery. *Environ. Adv.* 2, 100008. doi:10.1016/j.envadv.2020.100008.